

Supplementary Materials

Synergistic enhancement of lithium storage in biomass-derived hard carbon anodes via structure and phosphorus doping engineering

Hongbin Fei¹, Yuntao Yang¹, Taotao Zeng², Taoxin Tang¹, Liangliang Liu¹, Jiahao Wan^{3,4}, Yanhong Zou^{1,*}, Zeyan Zhou^{3,*}

¹School of Physics and Electronics, Hunan University, Changsha 410082, Hunan, China.

²College of Materials Science and Engineering, Changsha University of Science & Technology, Changsha 410114, Hunan, China.

³College of Materials Science and Engineering, Hunan Joint International Laboratory of Advanced Materials and Technology for Clean Energy, Hunan University, Changsha 410082, Hunan, China.

⁴Department of Materials Science and Engineering, Guangdong Technion-Israel Institute of Technology, Shantou 515063, Guangdong, China.

***Correspondence to:** Prof. Yanhong Zou, School of Physics and Electronics, Hunan University, Changsha 410082, Hunan, China. E-mail: yanhongzou@hnu.edu.cn; Dr. Zeyan Zhou, College of Materials Science and Engineering, Hunan Joint International Laboratory of Advanced Materials and Technology for Clean Energy, Hunan University, Changsha 410082, Hunan, China. E-mail: zhouzeyan@hnu.edu.cn

ORCID: Zeyan Zhou (0000-0002-4306-1677)

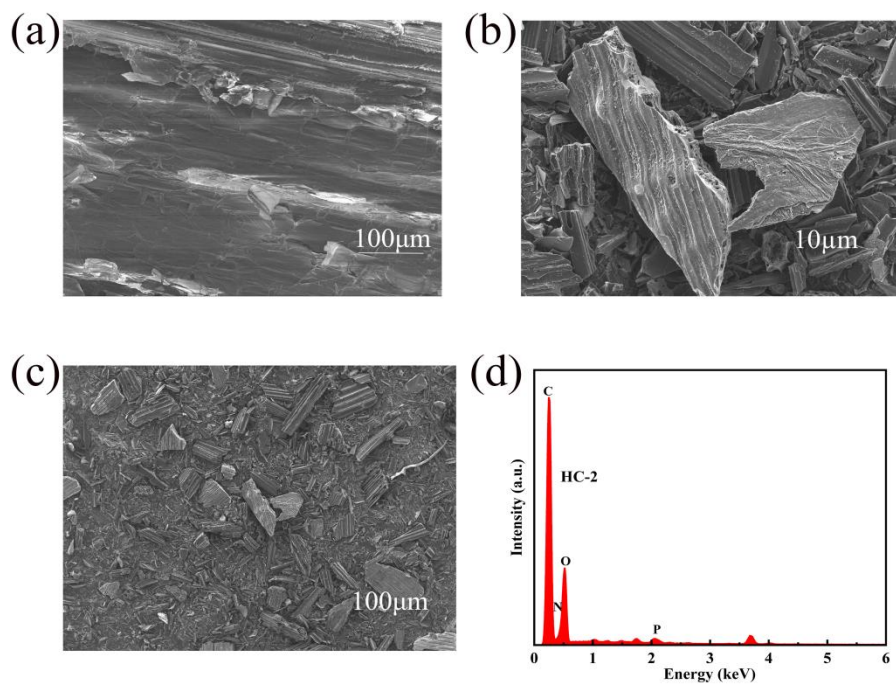


Fig. S1 (a) SEM image of OHC-2, (b-c) SEM images of HC-2 at different magnifications and (d) EDS image of HC-2.

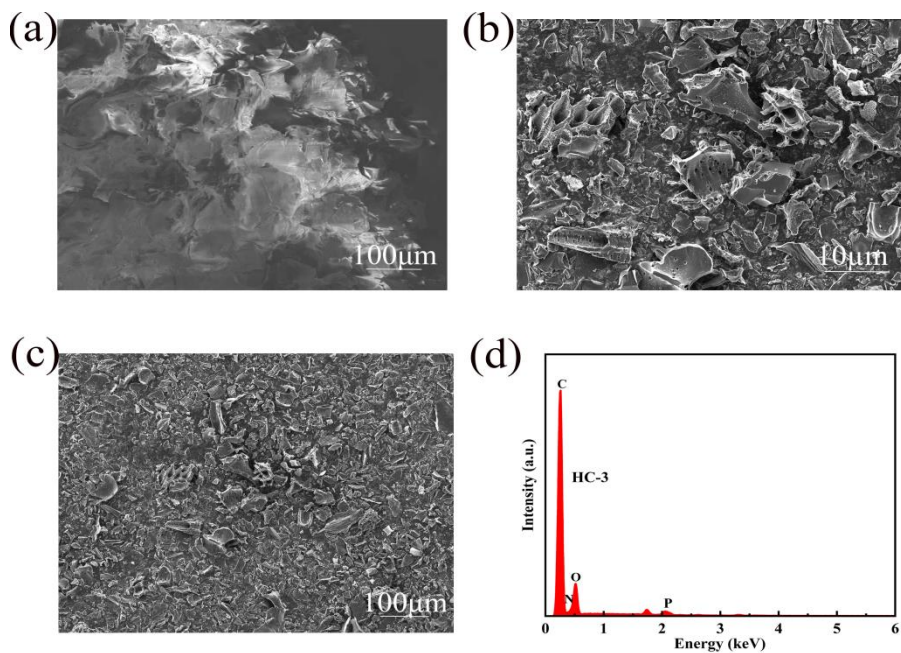


Fig. S2 (a) SEM image of OHC-3, (b-c) SEM images of HC-3 at different magnifications and (d) EDS image of HC-3.

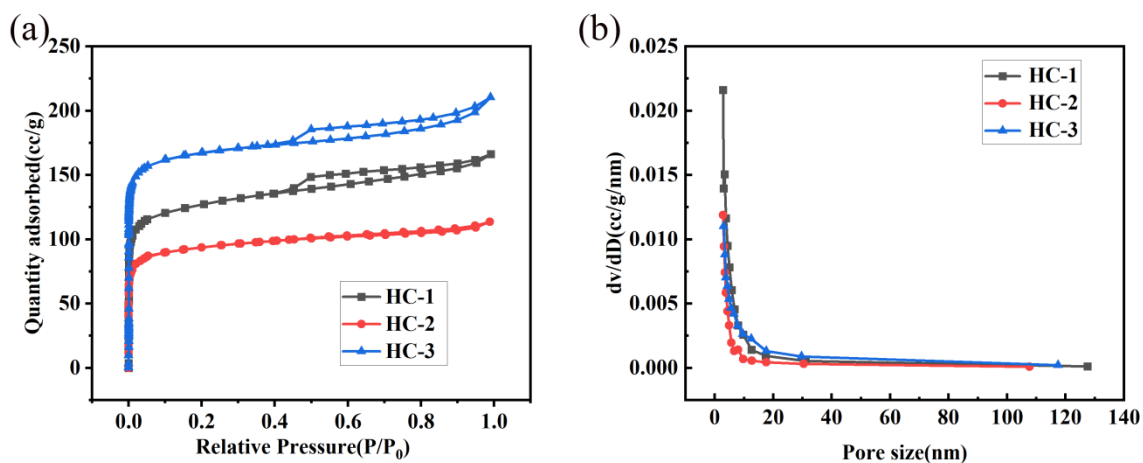


Fig. S3 (a) N₂ adsorption/desorption isothermal curves and (b) Pore size distribution function of these three hard carbon anode materials.

Table S1. Structural characteristic of hard carbon materials prepared by different precursor

Sample	BET surface area (m ² /g)	Total pore volume (cm ³ /g)	The average pore diameter(nm)
HC-1	474.00	0.086	2.78
HC-2	367.05	0.064	2.70
HC-3	656.91	0.114	4.21
HC-1-P5	491.70	0.110	1.89
HC-1-P10	632.55	0.115	1.95
HC-1-P15	786.30	0.212	2.11

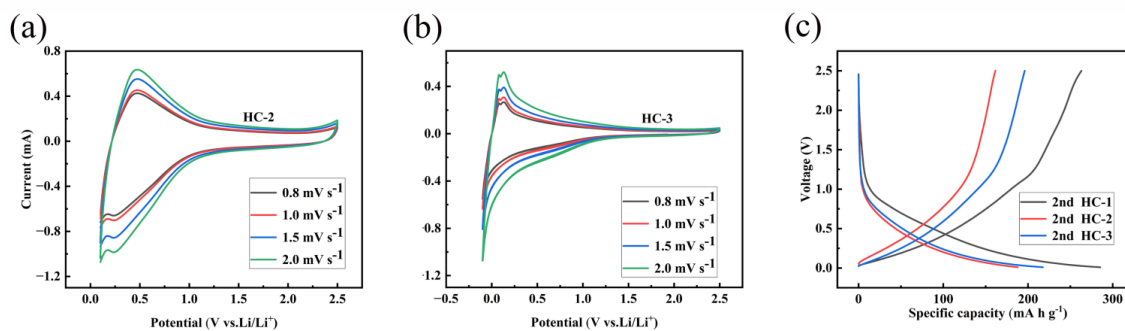


Fig. S4 (a-b) CV curves of HC-2 and HC-3 at different rates; (c) the second cycle galvanostatic charge/discharge curves of the three materials at 0.1 mA g⁻¹.

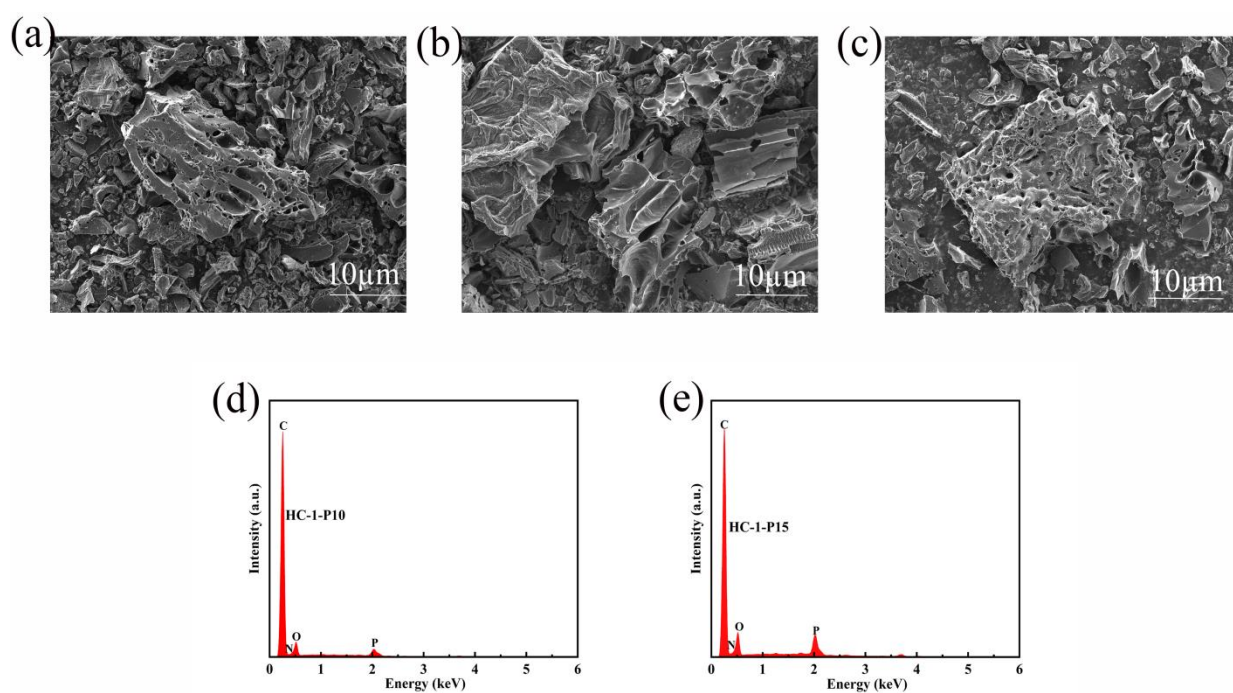


Fig. S5 (a-c) Small magnification SEM images of HC-1 at phosphorus contents of 5wt%, 10wt%, and 15wt%, respectively and (d-e) EDS images of HC-1-P10 and HC-1-P15.

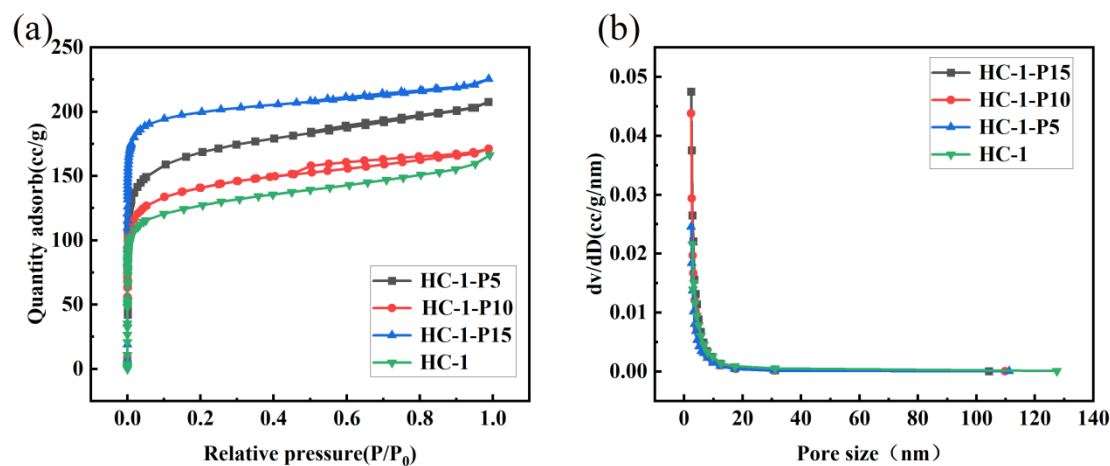


Fig. S6 (a) N₂ adsorption/desorption isothermal curves and (b) Pore size distribution function of HC-1 at phosphorus contents of 5wt%, 10wt%, and 15wt% respectively.

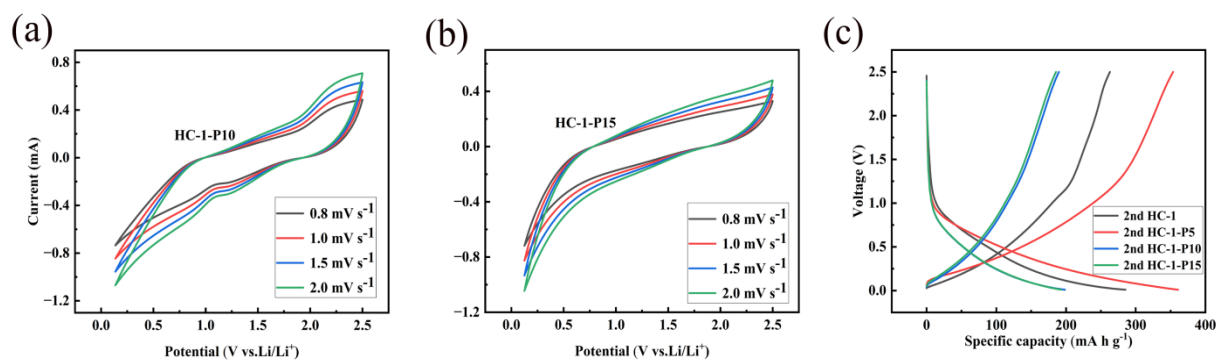


Fig. S7 (a-b) CV curves of HC-1-P10 and HC-1-P15 at different rates; (c) the second cycle galvanostatic charge/discharge curves of HC-1 at phosphorus contents of 5wt%, 10wt%, and 15wt% at 0.1 mA g⁻¹.